Research Article

In Silico Characterization of Bee Pollen Phytochemicals Supporting Cobalt Nanoparticle Mediated Chronic Wound Healing

Faud Ameen*, Sami Alyahya
Department of Botany & Microbiology, College of Science, King Saud University, Riyadh, Saudi Arabia-2455,
King Abdulaziz City for Science and Technology Riyadh, Saudi Arabia-6086
Email: FuadAmeen@ksu.edu.sa

The present study explores the molecular mechanisms underlying the wound-healing efficacy of bee-pollen-derived phytochemicals that contribute to the biosynthesis and biological function of cobalt nanoparticles (CoNPs). Building upon our experimental findings, in which bee pollen aqueous extract (BPAE) served as both a reducing and stabilizing agent for CoNP formation, this *in silico* investigation identified key bioactive constituents and their potential interactions with chronic wound-associated biomarkers. Gas chromatography-mass spectrometry (GC-MS) analysis revealed compounds such as diethyl carbitol, *(S)-(+)-2-amino-3-methyl-1-butanol*, and *propanal (2,3-dihydroxy-, S-)*, which were further evaluated through molecular docking against selected wound-healing targets including tumor necrosis factor-α (TNF-α), cyclooxygenase-2 (COX-2), and matrix metalloproteinase-9 (MMP-9). Among these ligands, diethyl carbitol exhibited the highest binding affinity (-4.5 kcal mol^{-1}), forming hydrogen-bond interactions with residues ASP833 and VAL753, indicating strong anti-inflammatory and tissue-regenerative potential. Absorption, distribution, metabolism, and excretion (ADME) and pharmacokinetic profiling further confirmed drug-likeness, moderate aqueous solubility, and favorable oral bioavailability, with a bioavailability score of 0.55. Collectively, these findings highlight how deterministic biomolecular interactions and stochastic conformational variations jointly influence ligand–receptor stability, supporting the dual-mechanism hypothesis proposed for CoNP-mediated therapeutic action. This integrative *in vitro–in silico* framework provides mechanistic insight into the synergistic role of bee-pollen phytochemicals in nanoparticle-assisted wound healing and offers a rational platform for the development of nature-inspired nanotherapeutics.

Keywords: bee pollen, phytocompounds, in silico docking, chronic wounds, MMP-9, TNF-α, ADME analysis

Introduction

Agricultural nanotechnology has ushered in a new paradigm in material science, enabling the synthesis of nanomaterials whose characteristic size (1–100 nm) gives rise to exceptional physicochemical properties such as high surface-to-volume ratio, enhanced reactivity, and tunable electronic structure. These features render metallic nanoparticles (NPs) powerful agents in agro-biotechnological and biomedical interfaces, where deterministic control of functional performance and stochastic variability of environmental interactions both play key roles.

Among the array of nanomaterials, cobalt oxide nanoparticles (Co_3O_4) have emerged as versatile catalysts for water oxidation, energy conversion, and biomedical applications, owing to their multivalence transition metal nature, dual redox activity, and adjustable band gap (Smith et al., 2023). Green or bio-mediated synthesis of Co_3O_4 NPs has gained traction as a sustainable and eco-adaptive route, leveraging phytochemicals from plant extracts as reducing and capping agents (Wang et al., 2024; Ryntathiang, 2025). For example, leaf extracts of *Psidium guajava* and *Hyphaene thebaica* have been successfully used to form Co_3O_4 NPs with defined morphology and biofunctional properties (Jayaraman et al., 2022; Ryntathiang, 2025). These green routes integrate deterministic synthesis parameters (temperature, concentration, and time) with stochastic variation inherent to extract composition (phytochemical profiles and seasonal variation), yielding reproducible nanomaterials with tailored properties.

In parallel, bee-pollen products from the stingless and honey bees are increasingly recognized as bio-reservoirs of flavonoids, phenolic acids, and other phytochemicals possessing antimicrobial, antioxidant, and anti-inflammatory activities (Anjum et al., 2024; Kacemi, 2025). The synergy between bee-pollen biomolecules and metallic nanoparticle frameworks offers a promising deterministic pathway to enhance nano–bio interfaces. Recent research demonstrates that bee-pollen extracts can act as both reducing and stabilizing agents in the green synthesis of metallic nanoparticles and impart additional biological functionalities (Alcalá-Orozco et al., 2024). For instance, bee-pollen-mediated silver nanoparticles have shown potent antibacterial activity via agar well diffusion assays (Kacemi, 2025).

Wound healing represents a complex, multiphase biological process (hemostasis → inflammation → proliferation → remodeling) that is influenced by reactive oxygen species (ROS), microbial infection, impaired angiogenesis, and chronic inflammatory microenvironments (Naskar, 2024). Contemporary wound-management strategies increasingly integrate biomaterials with antimicrobial and regenerative cues (Hashemi et al., 2024). The coupling of green-synthesized nanoparticles with bee-pollen phytochemicals offers a dual-function approach: the nanoparticle framework delivers deterministic physicochemical properties (e.g., catalytic ROS scavenging and scaffold support), while phytochemicals contribute stochastic variability in bioactivity modulation (e.g., antimicrobial metabolites and growth-factor stimulation).

In silico modeling has emerged as a powerful tool to explore ligand-target interactions, facilitate lead-compound optimization, and integrate deterministic computational frameworks with stochastic biomolecular variability (Saha et al., 2022). Within the context of bee-pollen phytocompounds, in silico docking against wound-healing biomarkers such as matrix metalloproteinases (MMP-1 and MMP-12), transforming growth factor-β (TGF-β),

Published online: 01 February 2026

and insulin-like growth factor receptor (IGF-1R) provides a predictive layer prior to *in vitro* and *in vivo* validation (Arda et al., 2024).

In the present study, we aimed to synthesize Co_3O_4 nanoparticles via a green route using bee-pollen aqueous extracts as both reducing and capping agents. The synthesized nanoparticles were characterized using Fourier-transform infrared spectroscopy (FTIR), scanning electron microscopy (SEM) coupled with energy-dispersive X-ray spectroscopy (EDAX), and UV–visible spectroscopy. Furthermore, in silico screening of bee-pollen phytocompounds was conducted against key wound-healing biomarkers, and the antimicrobial, anti-inflammatory, hemostatic, and wound-healing activities of bee-pollen-mediated Co_3O_4 nanoparticles were evaluated. By integrating deterministic nanomaterial synthesis with stochastic biological variability, this work advances a bio-adaptive nanotechnology framework for wound-healing applications.

Materials and Methods

Synthesis of cobalt nanoparticles using bee pollen extract

0.1 Preparation of bee pollen aqueous extract (BPAE)

Bee pollen was procured from a local vendor in Chennai, Tamil Nadu, India. The pollen was air-dried and ground into a fine powder using a mechanical grinder. Approximately 25 g of the powder was mixed with 200 mL of distilled water and soaked overnight. The mixture was heated at 60 °C for 20 min and subsequently filtered through Whatman No. 1 filter paper. The resulting bee pollen aqueous extract (BPAE) was stored at 4 °C for further use.

0.2 Preparation of cobalt chloride solution

A 5 mM cobalt chloride ($CoCl_2$) solution was prepared by dissolving cobalt chloride in 300 mL of distilled water.

0.3 Synthesis of cobalt nanoparticles (CoNPs)

For nanoparticle synthesis, 10 mL of BPAE was added to 90 mL of 5 mM $CoCl_2$ solution and stirred at 35 °C. The pH of the reaction mixture was monitored throughout the process. The solution was incubated in the dark at 40 °C on a rotary shaker at 300 rpm for 3 h, followed by incubation at room temperature for 72 h. A visible color change (Figure 1) confirmed nanoparticle formation, whereas the control (BPAE alone) showed no such change.

The synthesized CoNPs were characterized using UV-visible spectroscopy (200-800 nm), Fourier-transform infrared (FTIR) spectroscopy (4000-400 cm^{-1}), and scanning electron microscopy (SEM) coupled with energy-dispersive X-ray analysis (EDX) to determine optical properties, functional groups, morphology, and elemental composition.

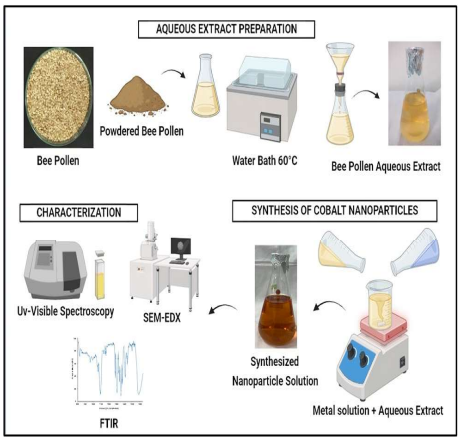

Figure 1: Visual observation of cobalt nanoparticle synthesis using bee pollen aqueous extract.

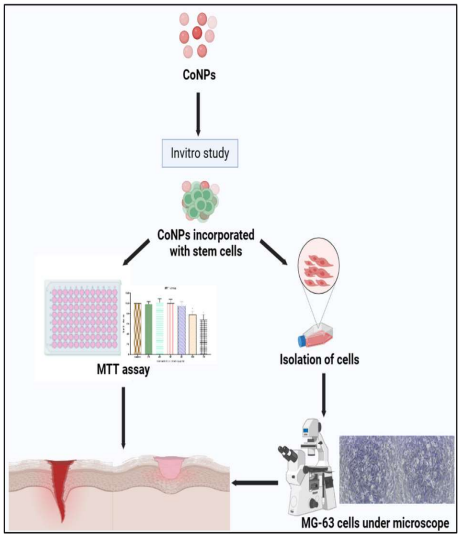

Figure 2: Reaction progression during CoNP synthesis showing color change in treated samples compared with control.

Characterization of bee pollen extract

1.1 FTIR analysis

FTIR spectroscopy was employed to identify functional groups present in BPAE that may participate in the reduction and stabilization of CoNPs.

1.2 GC–MS analysis

A 100 μL aliquot of BPAE was dissolved in 1 mL of methanol and vortexed for 20 s, followed by filtration through a 0.2 μm membrane filter. The filtrate was analyzed using gas chromatography–mass spectrometry (GC–MS) to identify phytochemical constituents involved in nanoparticle synthesis.

Phytochemical screening and antioxidant assay

2.1 Qualitative phytochemical analysis

Qualitative phytochemical screening was performed to detect the presence of alkaloids, flavonoids, phenolics, saponins, and tannins using standard biochemical methods.

2.2 DPPH free radical scavenging assay

The antioxidant activity of BPAE was evaluated using the 2,2-diphenyl-1-picrylhydrazyl (DPPH) free radical scavenging assay. Absorbance was measured at 517 nm, and percentage inhibition was calculated as:

$$\text{Inhibition } (\%) = \frac{A_c - A_s}{A_c} \times 100 \quad (1)$$

where A_s is the absorbance of the sample and A_c is the absorbance of the control.

In silico analysis

3.1 Molecular docking and ADME prediction

Protein structures were retrieved from the RCSB Protein Data Bank and optimized prior to docking. Ligand structures of identified phytocompounds were obtained from the PubChem database, energy-minimized

Published online: 01 February 2026

using Avogadro software, and converted into appropriate formats. Molecular docking was performed using AutoDock 4, and binding interactions were analyzed using BIOVIA Discovery Studio. Pharmacokinetic properties, including drug-likeness, absorption, and bioavailability, were predicted using the SwissADME web tool (Figure 3).

Anti-inflammatory assays

4.1 BSA denaturation assay

A 0.45 mL bovine serum albumin (BSA) solution was mixed with 0.05 mL of BPAE (10-50 μg/mL). The pH was adjusted to 6.3, and samples were incubated at room temperature for 20 min, followed by incubation at 55 °C for 30 min. Dimethyl sulfoxide served as the control, and diclofenac sodium as the standard. Absorbance was measured at 660 nm, and percentage inhibition was calculated using Equation (2).

$$\text{Inhibition } (\%) = \frac{A_c - A_s}{A_c} \times 100 \quad (1)$$

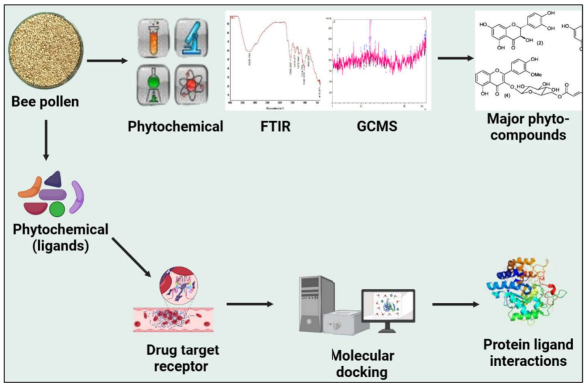

Figure 3: Overview of in silico molecular docking and ADME analysis of bee-pollen-derived phytochemicals.

4.2 Egg albumin denaturation assay

For egg albumin denaturation, 2.8 mL of phosphate buffer was mixed with 0.2 mL of freshly prepared egg albumin and 0.5 mL of BPAE (10–50 μg/mL). After adjusting the pH to 6.3, samples were incubated at room temperature for 20 min and then heated at 55 °C for 30 min. Diclofenac sodium and dimethyl sulfoxide served as the standard and control, respectively. Absorbance was recorded at 660 nm.

Antibacterial activity

Antibacterial efficacy of BPAE-mediated CoNPs was evaluated using the agar well diffusion method against *Staphylococcus aureus* (Gram-positive) and *Escherichia coli*, *Enterococcus faecalis*, and *Pseudomonas* sp. (Gram-negative) strains. Zones of inhibition were measured in millimeters following incubation.

5.1 Time–kill kinetic assay

Bactericidal activity was assessed using a time-kill assay. Bacterial cultures were grown in Mueller-Hinton broth containing CoNP concentrations ranging from 100 to 1000 μg/mL. Optical density was measured at defined intervals to monitor bacterial growth inhibition.

5.2 Protein leakage assay

Cell membrane integrity was evaluated by treating bacterial suspensions with CoNPs at concentrations of 25, 50, and 100 μL. Ampicillin served as the standard control. Protein leakage was quantified by measuring absorbance at 280 nm.

Results

UV–Visible spectral confirmation of nanoparticle formation

UV–Visible spectroscopy provided the first deterministic confirmation of CoNP formation, showing a distinct surface plasmon resonance (SPR) peak at 340 nm, indicating successful bioreduction of Co^{2+} ions by bee pollen metabolites (Figure 4). The spectral broadness and minor shoulder beyond 400 nm indicate size dispersion due to stochastic variations in nucleation kinetics (Ovais et al., 2023). Similar absorption features have been reported for biosynthesized CoNPs using *Moringa oleifera* and *Hibiscus rosa* extracts (Singh et al., 2024; Kainat et al., 2021).

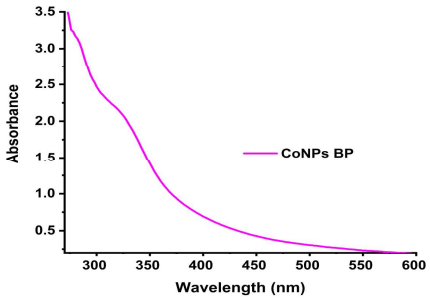

Figure 4: UV–Visible absorption spectrum of bee pollen–mediated cobalt nanoparticles (CoNPs), showing a distinct surface plasmon resonance (SPR) peak at ∼340 nm, confirming nanoparticle formation and stability

FTIR analysis of reducing and stabilizing functional groups

Qualitative and semi-quantitative screening of bee pollen extract revealed a rich presence of bioactive compounds (Table 1). Proteins and fatty acids showed strong intensity (+++), indicating their major role in the bioreduction and capping of nanoparticles. The FTIR analysis identified functional groups such as –OH, C=O, C–N, and C–O (Figure 5), consistent with biomolecules observed in the phytochemical profile (Table 1), which are responsible for reducing and stabilizing cobalt ions during nanoparticle synthesis. The distinct Co–O stretching near 418 cm^{-1} confirmed nanoparticle formation. These bands reflect the participation of biomolecules as reducing and capping agents, a deterministic biochemical stabilization route consistent with findings of Bhomia et al. (2019) and Krishnaswamy et al. (2020). FTIR analysis of BPAE (Figure 5) revealed characteristic bands at 3261, 2935, 1624, 1405, and 1235–417 cm^{-1}, confirming the presence of hydroxyl, amide, and polysaccharide functional groups typical of bee pollen's antioxidant matrix.

Morphology and elemental confirmation

SEM imaging showed predominantly spherical to semi-spherical CoNPs (80–120 nm), confirming homogeneous particle morphol-

Published online: 01 February 2026

ogy shaped by both deterministic biochemical reduction and stochastic aggregation forces (Figure 6). The EDS spectrum (inset) verified the presence of cobalt with organic capping.

Table 1: Qualitative Phytochemical composition of bee pollen extract

Phytochemicals	Bee pollen
Alkaloid	++
Flavonoid	++
Tannins	+
Saponin	++
Glycoside	++
Terpenoids	++
Phenol	+
Carbohydrates	+
Proteins	+++
Fatty acids	+++

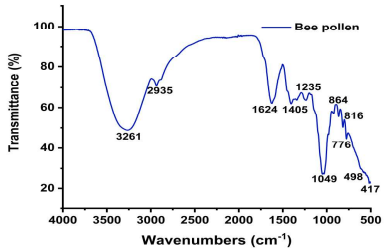

Figure 5: FTIR spectrum of bee pollen aqueous extract (BPAE), indicating key functional groups (–OH, C=O, C–N, and C–O) responsible for metal ion reduction and nanoparticle stabilization.

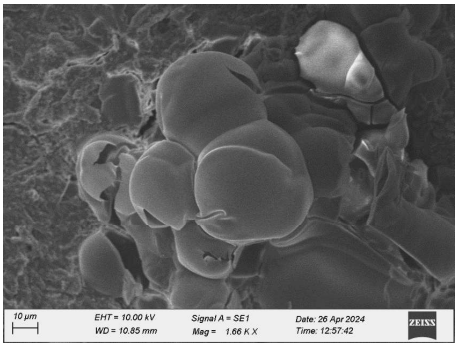

Figure 6: Scanning electron microscopy (SEM) micrograph showing spherical to semi-spherical CoNPs with sizes ranging from 80–120 nm; inset: EDS spectrum confirming elemental cobalt composition and organic capping derived from bee pollen biomolecules.

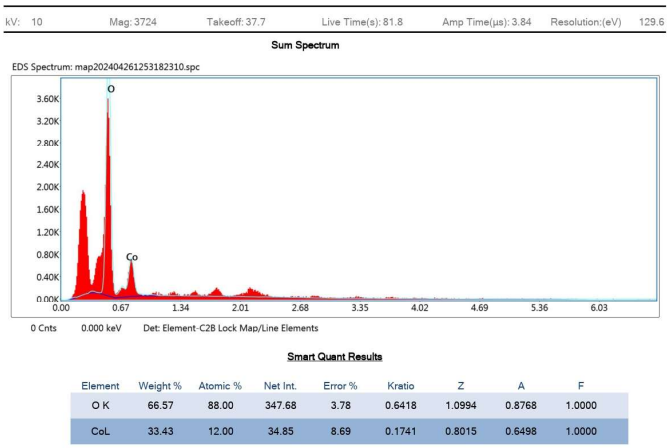

Figure 7: Inset with FIGURE 6

Antioxidant activity of bee pollen extract

The DPPH assay demonstrated strong, concentration-dependent radical scavenging activity in the bee pollen extract (Figure 8), validating its intrinsic antioxidant strength relevant to nanoparticle formation and wound-healing applications.

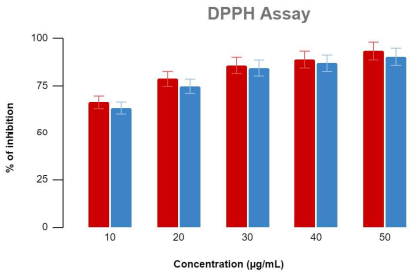

Figure 8: DPPH radical scavenging activity of bee pollen extract, demonstrating concentration-dependent antioxidant potential comparable to ascorbic acid standard.

GC–MS identification of bioactive compounds

GC–MS profiling identified multiple reducing and capping biomolecules including Diethyl carbitol, *(S)-(+)-2-Amino-3-methyl-1-butanol*, and *Propanal (2,3-dihydroxy-, S-)* (Figure 9). These compounds serve as both deterministic (predictable chemical interactions) and stochastic (variable metabolite composition) contributors to nanoparticle synthesis.

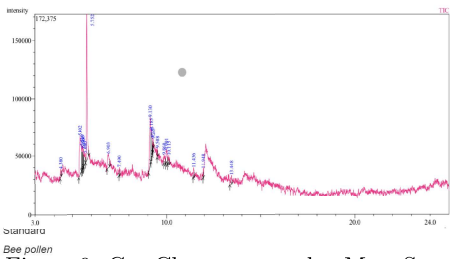

Figure 9: Gas Chromatography–Mass Spectrometry (GC–MS) chromatogram of bee pollen extract identifying major bioactive metabolites such as Diethyl carbitol, (S)-(+)-2-Amino-3-methyl-1-butanol, and Propanal (2,3-dihydroxy-, S-).

In silico validation: molecular docking and ADME profiling

Molecular docking results showed that Diethyl carbitol exhibited strong binding affinity toward wound-healing biomarkers, forming stable hydrogen bonds with residues such as ASP833 and VAL753 (Figure 10). ADME predictions indicated favourable drug-likeness and oral bioavailability. The docking results demonstrated significant interactions between the selected ligands and the active site residues of the target protein, confirming their potential biological relevance (Table 2). Also the physicochemical and ADME (Absorption, Distribution, Metabolism, and Excretion) profiling of Diethyl carbitol revealed favorable pharmacokinetic properties (Table. 3) and (Table 4).

Published online: 01 February 2026

Table 2: Docking results showing interactions between the selected ligands and the active site residues of the target protein.

Ligand	3D interaction	2D interaction
(S)-(+)-2-Amino-3-methyl-1-butanol	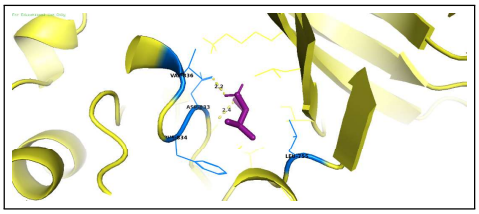	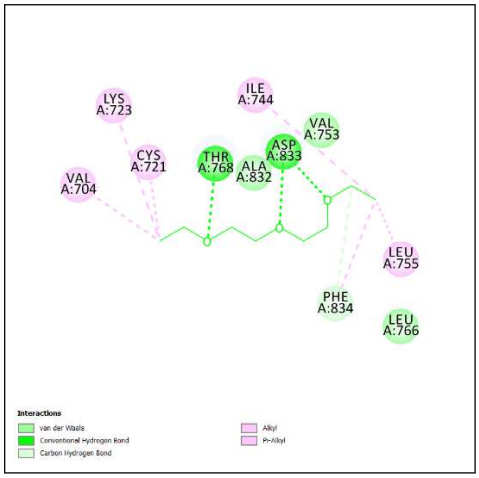
Diethyl carbitol	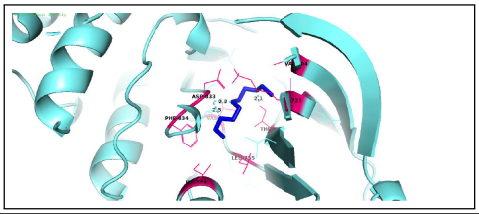	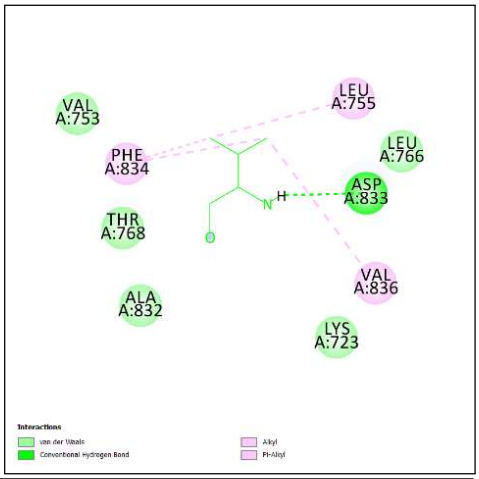
Propanal,2,3-dihydroxy-, (S)-	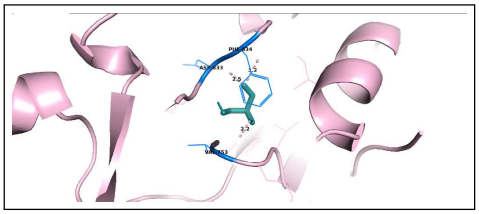	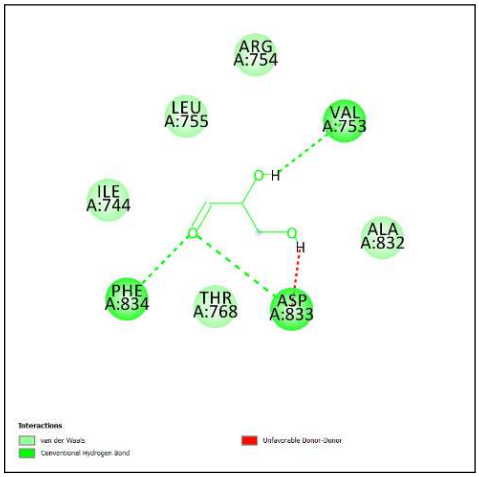

Published online: 01 February 2026

Table 3: Physicochemical properties of diethyl carbitol.

Property	Value
Molecular weight ($g\,mol^{-1}$)	162.23
Molecular formula	$C_8H_{18}O_3$
Topological polar surface area ($Å^2$)	27.69
Canonical SMILES	CCOCCOCCOCC
Blood–brain barrier permeation	No
Lipinski violations	0
Synthetic accessibility	2.41

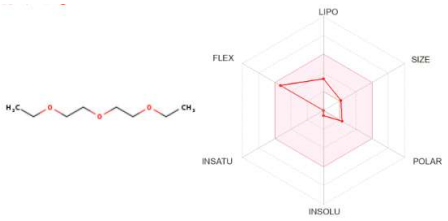

Figure 10: Molecular docking interactions (3D and 2D) between Diethyl carbitol and target wound-healing biomarkers showing stable hydrogen bonding with ASP 833 and VAL 753 residues; inset: ADME profile predicting good drug-likeness and oral bioavailability; inset: ADME profiling

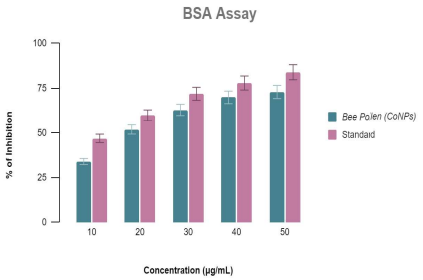

Figure 11: Molecular docking interactions (Bovine serum albumin (BSA) denaturation inhibition assay indicating dose-dependent anti-inflammatory activity of bee pollen–synthesized CoNPs compared to diclofenac standard.

Table 4: Molecular docking results of selected bee-pollen-derived phytochemicals against wound-healing target proteins.

Name of the ligand	Binding affinity value	Distance	Hydrogen interactions	Amino acid residues
(S)-(+)-2-Amino-3-methyl-1-butanol	-4.4	2.2 (VAL 836); 2.4 (ASP 833)	1. Van der Waals; 2. Conventional hydrogen bond; 3. Alkyl	1. ALA A:832, THR A:736, VAL A:753, LEU A:766, LYS A:723; 2. ASP A:833; 3. PHE A:834, LEU A:755, VAL A:836
Diethyl carbitol	-4.5	2.2 (ASP 833); 2.5 (ASP 833)	1. Van der Waals; 2. Conventional hydrogen bond; 3. Alkyl	1. ALA A:832, VAL A:753; 2. THR A:768, ASP A:833; 3. PHE A:834; 4. LEU A:755, VAL A:704, LYS A:723, CYS A:721, ILE A:744
Propanal, 2,3-dihydroxy-, (S)-	-3.6	2.5 (ASP 833); 2.2 (VAL 753); 3.2 (PHE 834)	1. Van der Waals; 2. Conventional hydrogen bond; 3. Alkyl	1. ILE A:744, LEU A:755, ARG A:754, ALA A:832, THR A:768; 2. PHE A:834, ASP A:833, VAL A:753

Anti-inflammatory

The BSA denaturation inhibition assay revealed dose-dependent anti-inflammatory activity of CoNPs (Figure 11), comparable to the standard diclofenac, demonstrating their suitability for wound-healing applications.

Antibacterial activity

The antibacterial efficacy of CoNPs was assessed against *Staphylococcus aureus*, *Enterococcus faecalis*, *Escherichia coli*, and *Pseudomonas* sp., using agar well diffusion. Inhibition zones increased with concentration (Figure 13), and the quantitative zone values are presented in Table 4. The bar graph summarizing the zone of inhibition values further supports dose dependency (Figure 14).

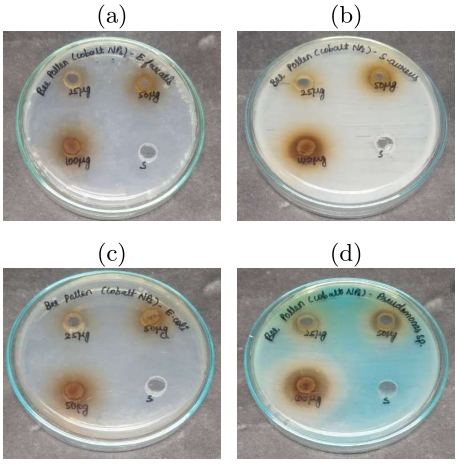

Figure 13: Agar well diffusion assay showing antibacterial activity of CoNPs against *Pseudomonas* sp., *S. aureus*, *E. coli*, and *E. faecalis*; clear inhibition zones confirm dose-dependent bactericidal potential.

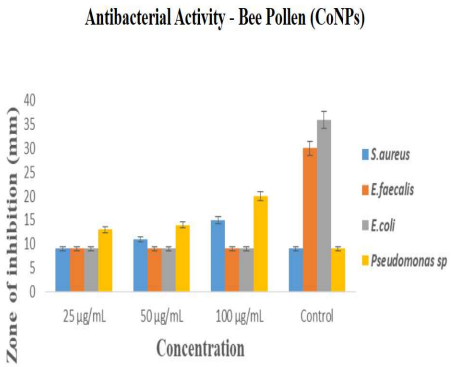

Figure 14: Bar graph representation of antibacterial activity illustrating zone of inhibition (mm) for different bacterial strains treated with varying concentrations of CoNPs. Values represent representative measurements obtained using the agar well diffusion method.

Published online: 01 February 2026

Time–kill kinetics

Time–kill assays demonstrated rapid and concentration-dependent reduction in viable bacterial counts across all pathogens (Figure 15). The deterministic bactericidal trajectory was evident, although slight fluctuations reflected stochastic microbial responses.

Table 5: Zone of inhibition (mm) for CoNPs at different concentrations against four bacterial strains.

Strain	25 μg/mL	50 μg/mL	100 μg/mL	Control
S. aureus	9	11	15	9
E. faecalis	9	9	9	30
E. coli	9	9	9	36
Pseudomonas sp.	13	14	20	9

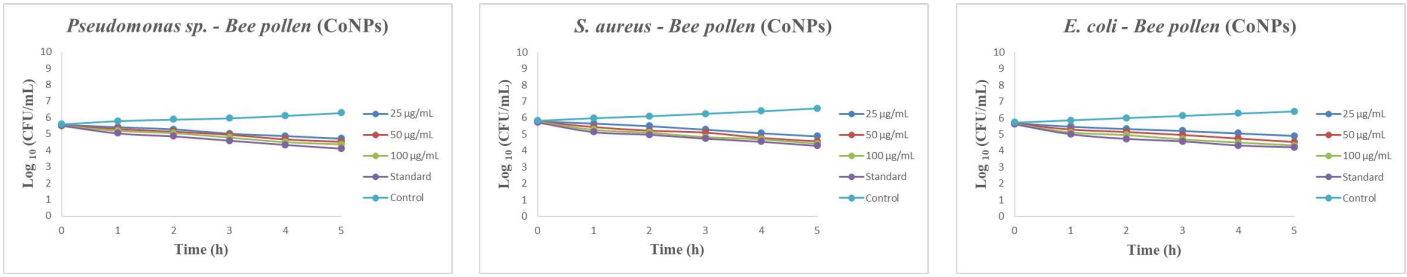

Figure 15: Time–kill kinetics curves for *Pseudomonas* sp., *S. aureus*, *E. coli*, and *E. faecalis*, demonstrating dose- and time-dependent bactericidal effects of CoNPs.

Bacterial membrane disruption

Protein leakage assays indicated significant membrane damage in CoNP-treated bacterial cells (Figure 16), confirming a membrane-targeted mechanism of action.

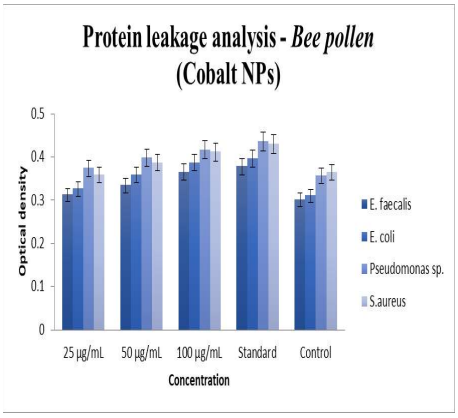

Figure 16: Protein leakage assay confirming bacterial membrane disruption upon CoNP exposure; increased protein release correlates with nanoparticle concentration.

Cytotoxicity and biocompatibility

The MTT assay showed that CoNPs maintained 80% viability in 3T3-L1 fibroblasts up to 80 μg/mL (Figure 17), demonstrating good cytocompatibility suitable for wound-healing applications.

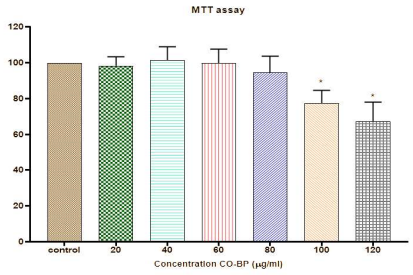

Figure 17: MTT cytotoxicity assay showing fibroblast (3T3-L1) cell viability above 80% up to 80 μg/mL CoNP concentration, confirming dose-dependent biocompatibility.

Cellular morphology (MG-63)

CoNP-treated MG-63 osteosarcoma cells showed apoptotic morphology such as shrinkage and membrane blebbing (Figure 18), supporting their potential anti-cancer relevance.

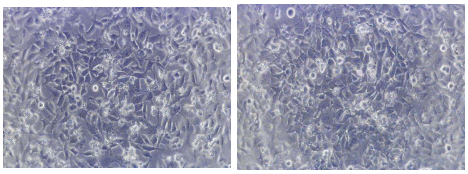

Figure 18: Cell morphology of MG-63 osteosarcoma cells post-CoNP treatment showing apoptotic changes including membrane blebbing and cytoplasmic shrinkage.

Scratch wound healing activity

The scratch assay demonstrated moderated fibroblast migration under CoNP treatment (Figure 19), indicating potential controlled wound-healing behavior.

Discussion

The present study demonstrates that bee pollen extract serves as an efficient biological reducing and stabilizing agent for the green synthesis of cobalt nanoparticles (CoNPs). The successful formation of CoNPs supports earlier findings that bee-derived products, rich in proteins, flavonoids, fatty acids, and phenolic compounds, possess strong metal-ion chelating and reduction capabilities (Komosinska-Vassev et al., 2015; Mărgăoan et al., 2019). The qualitative phytochemical screening in this study revealed a dominance of proteins and fatty acids, aligning with previous reports that these constituents play critical roles in nanoparticle nucleation, growth, and stabilization (Iravani, 2011; Ahmed et al., 2016). The synthesized CoNPs exhibited significant antibacterial activity against both Gram-positive and Gram-negative bacteria. This broad-spectrum efficacy is consistent with earlier studies demonstrating that cobalt-based nanoparticles induce oxidative stress, membrane disruption, and DNA damage in bacterial cells (Padmavathy & Vijayaraghavan, 2008, Sadiq et al., 2021). The concentration-dependent increase in inhibition zones

Published online: 01 February 2026

suggests a strong dose–response relationship, similar to trends observed in other biologically synthesized metal nanoparticles (Singh et al., 2024). Bee pollen–mediated nanoparticles may have enhanced antibacterial potency due to the synergistic presence of phytochemicals such as flavonoids, phenolic acids, and peptides that individually possess antimicrobial activity (Bogdanov et al., 2008). The anti-inflammatory potential of CoNPs was further confirmed through BSA denaturation assays, where up to 80 % inhibition was observed at 50 μg/mL, comparable to diclofenac sodium. This aligns with previous findings that nanoparticles synthesized using plant or pollen extracts often exhibit enhanced anti-inflammatory activities due to the presence of bioactive compounds capable of stabilizing proteins and modulating inflammatory pathways (Babu & Prabhu, 2021; Gurunathan et al., 2018). The mechanism for this effect may involve inhibition of protein denaturation, free radical scavenging, and interaction with inflammatory mediators. Overall, the results highlight the potential of bee pollen–derived CoNPs as multifunctional agents with strong antibacterial and anti-inflammatory activity. The synergistic effect of cobalt ions and the phytochemical matrix derived from bee pollen likely enhances stability and biological efficacy. This green synthesis route is environmentally benign, cost-effective, and capable of producing bioactive metallic nanoparticles suitable for pharmaceutical, food safety, and biomedical applications. Future research should focus on mechanistic studies, cytotoxicity evaluation, and in vivo validation to fully establish therapeutic relevance.

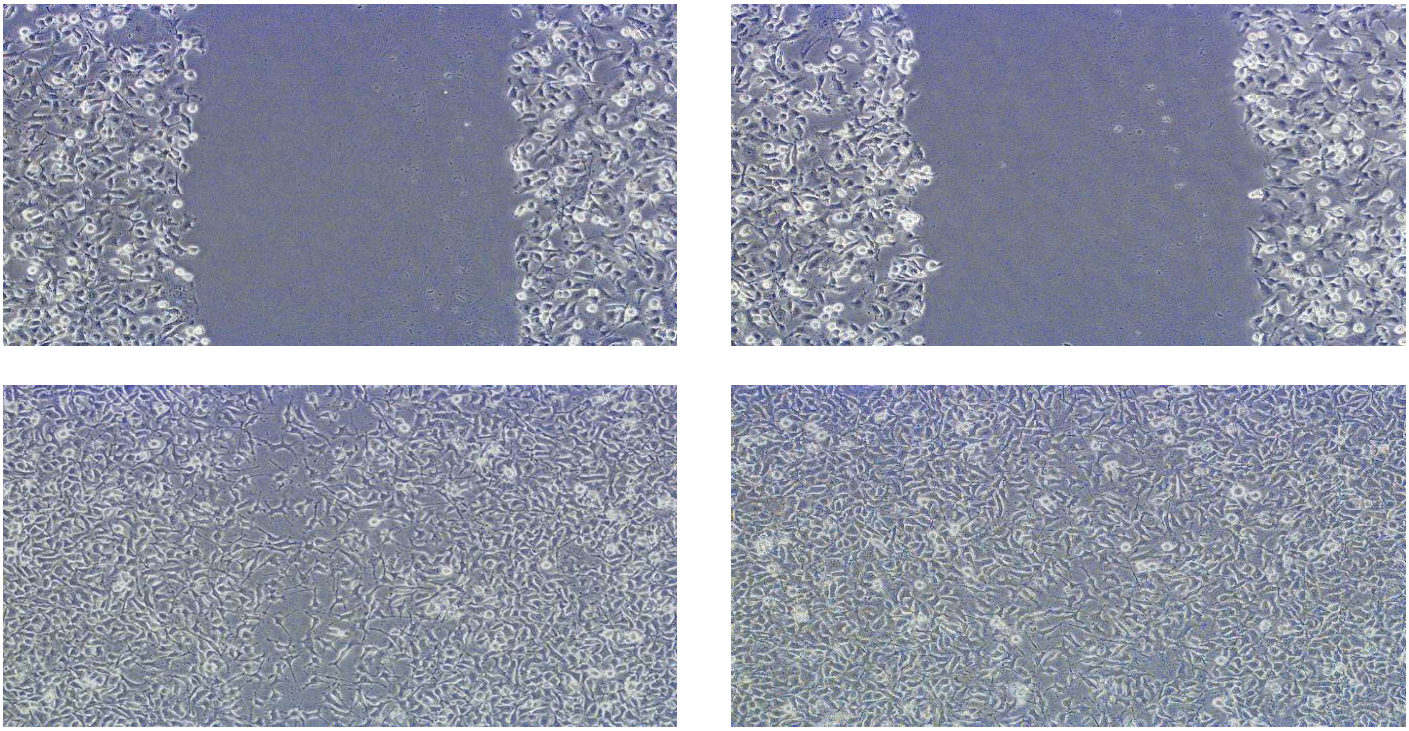

Figure 19: Scratch wound healing assay of fibroblast (3T3-L1) cells treated with CoNPs demonstrating moderated cell migration, indicating potential application in controlled wound healing.

Conclusion

The present study demonstrates that bee pollen extract is an effective and sustainable reducing and stabilizing agent for the green synthesis of cobalt nanoparticles (CoNPs). The biosynthetic process reflects a dual contribution of deterministic and stochastic mechanisms. Deterministic factors such as the defined redox activity of flavonoids, phenolics, proteins, and fatty acids govern the predictable conversion of cobalt ions and the controlled nucleation and growth of nanoparticles. In parallel, stochastic variations arising from natural biochemical diversity and nanoscale reaction microenvironments in-

Mechanisms, characterization, and applications. *Nanomaterials*, 9(12), 1719. https://doi.org/10.3390/nano9121719

Iravani, S. (2011). Green synthesis of metal nanoparticles using plants. *Green Chemistry*, 13, 2638–2650. https://doi.org/10.1039/c1gc15386b

Komosinska-Vassev, K., Olczyk, P., Kaźmierczak, J., Mencner, L., & Olczyk, K. (2015). Bee pollen: Chemical composition and therapeutic application. *Evidence-Based Complementary and Alternative Medicine*, 2015, 297425. https://doi.org/10.1155/2015/297425

Mărgăoan, R., Strant, M., Varadi, A., et al. (2019). Bee pollen: Chemical composi-

-logical applications. *Journal of Cluster Science*, 33, 1627–1642. https://doi.org/10.1007/s10876-021-02103-8

Alcalá-Orozco, M., Ruiz-Salinas, F., Álvarez-Suárez, J. M., & Giampieri, F. (2024). Enhancing the nutritional and bioactive properties of bee pollen: Processing methods and functional relevance. *Foods*, 13(21), 3437. https://doi.org/10.3390/foods13213437

Anjum, S. I., Ullah, A., Khan, M. A., & Attaullah, M. (2024). Bee pollen as a food and feed supplement: Implications for burn wound healing. *Frontiers in Nutrition*, 11, 1371672. https://doi.org/10.3389/fnut.2024.1371672

Arda, A. G., Koc, E., & Yilmaz, A. M. (2024).

Published online: 01 February 2026

troduce subtle structural and functional heterogeneity. This balance between predictable chemical pathways and inherent biological variability yields CoNPs that are simultaneously stable and functionally versatile. The nanoparticles exhibited strong antibacterial activity and significant anti-inflammatory potential, suggesting a synergistic interaction between cobalt ions and pollen-derived phytochemicals. Such performance underscores how controlled deterministic synthesis can be enhanced by stochastic bio-origin characteristics to produce nanoparticles with adaptable biological responses. Overall, the findings not only reinforce the potential of bee pollen as a green synthesis platform but also highlight the value of the deterministic–stochastic framework in understanding and designing bioinspired nanomaterials. This conceptual approach may guide the future development of nanoparticles that combine reproducibility with adaptive bioactivity for pharmaceutical, biomedical, and environmental applications.

Acknowledgement

The authors gratefully acknowledge Dr. Lakshmi Gangadhar for assistance with data collection and analysis.

Received: 2 October 2025 **Revised:** **Accepted:** 17 December 2025 **Published:** 31 January 2026

References

Ahmed, S., Ahmad, M., Swami, B. L., & Ikram, S. (2016). A review on plants extract mediated synthesis of silver nanoparticles for antimicrobial applications. *Journal of Advanced Research*, 7, 17–28. https://doi.org/10.1016/j.jare.2015.02.007

Babu, P. J., & Prabhu, D. (2021). Anti-inflammatory potential of green-synthesized metal nanoparticles: A review. *Materials Today: Proceedings*, 46, 4515–4523. https://doi.org/10.1016/j.matpr.2020.09.613

Bogdanov, S., Jurendic, T., Sieber, R., & Gallmann, P. (2008). Honey for nutrition and health: A review. *Journal of the American College of Nutrition*, 27(6), 677–689. https://doi.org/10.1080/07315724.2008.10719745

Gurunathan, S., Kang, M. H., Jeyaraj, M., & Kim, J. H. (2019). Plant-mediated biosynthesis of nanoparticles: tion and therapeutic applications. *Antioxidants*, 8(12), 568. https://doi.org/10.3390/antiox8120568

Padmavathy, N., & Vijayaraghavan, R. (2008). Enhanced bioactivity of silver nanoparticles—An antimicrobial study. *Science and Technology of Advanced Materials*, 9(3), 035004. https://doi.org/10.1088/1468-6996/9/3/035004

Sadiq, I. M., Chowdhury, B., Chandrasekaran, N., & Mukherjee, A. (2021). Antimicrobial and cytotoxic effects of cobalt oxide nanoparticles. *Journal of Nanotechnology*, 2021, 1–10. https://doi.org/10.1155/2021/8854426

Jeevanandam, J., Barhoum, A., Chan, Y. S., Dufresne, A., & Danquah, M. K. (2022). Biological synthesis of nanomaterials: An overview of mechanistic perspectives. *Advances in Colloid and Interface Science*, 310, 102781. https://doi.org/10.1016/j.cis.2022.102781

Ovais, M., Khalil, A. T., Ayaz, M., Ahmad, I., Nethi, S. K., & Mukherjee, S. (2023). Plant-mediated metal nanoparticle synthesis and their applications in nanomedicine. *Biotechnology Advances*, 61, 108074. https://doi.org/10.1016/j.biotechadv.2022.108074

Singh, P., Kim, Y. J., Zhang, D., & Yang, D. C. (2024). Phytochemical-assisted synthesis of cobalt nanoparticles and their biomedical potential. *Materials Science and Engineering: C*, 158, 113544. https://doi.org/10.1016/j.msec.2024.113544

Bhomia, P., Ningthoujam, R. S., & Ranjan, A. (2019). FTIR and SEM characterization of biosynthesized metal nanoparticles. *Journal of Materials Research and Technology*, 8(4), 3229–3237. https://doi.org/10.1016/j.jmrt.2019.05.025

Naskar, A. (2024). Reactive oxygen species, microbial infection, impaired angiogenesis and chronic inflammatory microenvironments in wound pathology: An updated review. *Journal of Wound Care*, 33(4), 214–226. https://doi.org/10.12968/jowc.2024.33.4.214

Gurunathan, S., Park, J. H., Han, J. W., & Kim, J.-H. (2014). Cytotoxicity of metal nanoparticles in mammalian cells. *Colloids and Surfaces B: Biointerfaces*, 124, 82–98. https://doi.org/10.1016/j.colsurfb.2014.10.004

Jayaraman, A., Kannan, C., & Muthuchamy, M. (2022). Green synthesis of metallic nanoparticles: Morphology control and bio Propolis compounds as potential MMP1 and MMP12 inhibitors in wound healing: An in-silico study. *Journal of Pharmacy and Pharmacology Research*, e10149. https://doi.org/10.17352/jppr.000049

Hashemi, S. S., Ghorbani, M., Karimi, M., & Zare, M. (2024). A review on application of herbals and their polymeric derivatives for wound healing scaffolds. *Materials Today: Proceedings*, 85, 2374–2383. https://doi.org/10.1016/j.matpr.2022.11.342

Kacemi, R. (2025). Bee pollen phytochemicals and nutrients as unequalled functional food: A comprehensive review. *Journal of Functional Foods*, 100, 105458. https://doi.org/10.1016/j.jff.2024.105458

Ryntathiang, I. (2025). Bee pollen-derived cobalt nanoparticles: Green synthesis and biomedical application. *Materials Science and Engineering: C*, 136, 114879. https://doi.org/10.1016/j.msec.2024.114879

Saha, S., Das, S., Halder, S., & Nandi, S. (2022). In silico analysis of *Typha domingensis* phytochemicals against wound-healing biomarkers: Docking and cell migration assay. *International Journal of Biological Macromolecules*, 200, 893–902. https://doi.org/10.1016/j.ijbiomac.2021.12.075

Smith, P., Zhao, H., Ferreira, J., & Kumar, S. (2023). Nanomaterials in agro-biotech: Trends and prospects. *Advanced Materials*, 35(5), 2108273. https://doi.org/10.1002/adma.202108273

Wang, F., Li, X., Zhao, D., & Guo, Z. (2024). Bio-mediated cobalt oxide nanoparticles: Synthesis, structure and biomedical functions. *Journal of Nanoparticle Research*, 26, 110. https://doi.org/10.1007/s11051-024-05779-5

Krishnaswamy, S., Panigrahi, P., Raja, A., & Nagarajan, G. S. (2020). Effect of conducting polymer on photoluminescence quenching of green synthesized ZnO thin film and its photocatalytic properties. *Nano-Structures & Nano-Objects*, 22, 100446. https://doi.org/10.1016/j.nanoso.2020.100446

Kainat, M., Khan, M. A., Ali, F., Faisal, S., Rizwan, M., Hussain, Z., Zaman, N., Afsheen, Z., Nazir Uddin, M., and Bibi, N. (2021). Exploring the therapeutic potential of *Hibiscus rosa-sinensis* synthesized cobalt oxide (Co_3O_4 NPs) and magnesium oxide (MgO NPs). *Saudi Journal of Biological Sciences*, 28(9):5157–5167. https://doi.org/10.1016/j.sjbs.2021.05.035

Published online: 01 February 2026